Comparison of Frank-Wolfe Variants for White-Box Adversarial Attacks

Tanner Aaron Graves - 2073559   Alessandro Pala - 2107800

June 2024

1   Abstract

With deep neural networks becoming ubiquitous in application, adversarial attacks have received much attention, as it has proved remarkably easy to create adversarial examples- genuine data that undergoes a minimal and unobtrusive corruption process in order to maximally harm the performance of a model. Access to a models architecture can enable white-box attacks, where gradients of loss with respect to input examples are exploited to create adversarial examples. The requirement that examples be minimally perturbed is a constraint on the optimization. The ability of Frank-wolf and variants have gathered much attention for their ability to be efficiently create adversarial examples while staying in a constraint set. In the paper we introduce discuss the application of Frank-Wolfe and two variants to this non-convex constrained optimization problem. Furthermore we discuss popular optimizations and their effect convergence and attack efficacy, comparing performance on attacks on models trained on MNSIT, FashionMNIST, and CFAIR-10 datasets. Finally, there is a discussion of the theoretical underpinnings of each algorithm.

2   Introduction

Adversarial attacks on CNNs are often stated as the following constrained optimization problem:

$$
\begin{aligned}
\min_{x} \quad & f(x) \\
\text{s.t.} \quad & ||x||_p \leq \epsilon
\end{aligned}
\tag{1}
$$

In the case of untargeted attacks on a classifier, we perturb an example with the aim it be incorrectly predicted as any other class. Here $f(x)$ is the loss function of the attacked model $-\ell(x, \hat{y})$. In the case of targeted attacks, we aim to maximize the likelihood of another class $y \neq \hat{y}$. The cost then is $f(x) = \ell(x, y)$. We have implemented both targeted and untargeted attacks, and come to focus on targeted attacks as the algorithms are seen to require more iterations to converge. The L_p constraint $||x||_p \leq \epsilon$ directly restricts the size of perturbations

made the to the example. An inherent problem of DNNs is often attacks can be consistently successful even with very small, even imperceptible ϵ. Different choices of p may be made giving $||x||_p = (\sum_i x_i^p)^{1/p}$. We have implemented and provide results for the L_2 and the $L_\infty(x) = \max_i |x_i|$ norms, focusing mostly on the ladder. We define the constraint set $\mathcal{M} = \{x : L_p(x) \leq \epsilon\}$. Of particular note is when $\mathcal{M}$ is a polytope, as is the case when $p \in \{1, \infty\}$. This corresponds to models making perturbations that are either sparse or have a maximal disturbance along each element. In these cases, the constraint set can be expressed as the convex combination of a finite set of vertices $\mathcal{M} = \text{Conv}\{\mathcal{A}\}$. This will be of particular relevance in the discussion of Away-step and pairwise variants. Otherwise, $\mathcal{A}$ is taken to be the boundary of $\mathcal{M}$. The constrained nature of this problem limits the applicability of a method like gradient descent, and requires integrating knowledge of the constraint space for effective optimization. Methods like Fast Signed Gradient attacks and projected gradient descent are popular choices, but either create unsophisticated adversarial examples or require wasteful projection onto the constraint space.

We explore Frank-Wolfe variants which are well suited to this problem by ensuring feasibility within the constraint set at each iteration with the efficient solving of a Linear Minimization Oracle (LMO).

$$LMO_\mathcal{A}(\nabla f(x_t)) \in \arg\min_{x \in \mathcal{A}} \langle \nabla f(x_t), x \rangle$$

The LMO is responsible for solving what is called the "Frank-Wolfe Subproblem" and at each iteration provides and optimal s_t such that updating x_{t+1} to move in the direction of s_t will remain in $\mathcal{M}$ Given it moves no more than some maximum step-size. By solving the LMO efficiently, the algorithm ensures that each iteration makes significant progress towards the optimal solution while respecting the constraints, thereby maintaining feasibility and accelerating convergence. Efficient solving of the LMO requires exploiting the structure of the constraint set $\mathcal{M}$. In the case of the L_∞ norm it has closed form solution:

$$LMO_\mathcal{A} = s_t = -\epsilon \, \text{sign}(\nabla f(x_t)) + x_0$$

This is clearly of $O(n)$ complexity where n is the number of elements in the gradient. This can be interpreted as defining an attack direction where each element is the maximum allowable perturbation $\pm\epsilon$ according to the gradient. With one iteration, this is exactly the outcome of a Fast Signed Gradient Attack. At each iteration, we can see that the LMO will give a vertex on the boundary of the constraint set $\mathcal{M}$ which was optimally chosen to be as close to the true gradient as possible while permitting subsequent iterations stay within the feasible set.

The constrained nature of the Adversarial Attack problem means that the norm of the gradient $||\nabla_x f(x)||$ is not a suitable convergence criterion, as boundary points need not have zero gradient. Instead, we adopt the Frank-Wolfe gap as a measure of both optimality and point feasibility. In the convex case, this gap measures the maximum improvement over the current iteration x_t within

the constraints $\mathcal{M}$ and is defined as:

$$g_t^{\text{FW}} := \max_{s \in \mathcal{M}} \langle x_t - s, \nabla f(x_t) \rangle = \langle -\nabla f(x_t), d_t^{\text{FW}} \rangle$$

The Frank-Wolfe gap g_t^{FW} is always non-negative $g_t^{\text{FW}} \geq 0$ and is zero if and only if x_t is a stationary point. This makes it a useful convergence criterion, particularly since stationary points need not have zero gradients in constrained problems. We found that $g_t^{\text{FW}} < 0.1$ to be a good convergence criterion for our models. In most circumstances, seccessful attacks will happen before this threshold. However, setting it higher seems to adversly effect attack success rate, and setting it lower is seen to require many more unneeded iterations. We cap the maximum iterations at 20 in this work.

The loss functions of Deep Neural Networks (DNNs), which are commonly the subject of adversarial attacks, are highly non-convex. Thus, the convergence of Frank-Wolfe methods in these applications is complicated by the fact that we are not guaranteed to find a global optimum or a successful attack, but rather convergence to a stationary point. It is also worth noting that, in the context of adversarial attacks, the Frank-Wolfe gap serves as an imprecise surrogate for success. In many cases, Frank-Wolfe methods generate successful attacks several iterations before convergence. This is because achieving an incorrect class probability higher than the correct class is often sufficient for a successful attack, whereas convergence indicates the new output class probability has been maximized.

3 Algorithms

We implement the original FW algorithm and amodified version with momentum FW with momentum [2]. We then compare the performance of these models with 2 variants [6]: Away Step Frank Wolfe, and Pairwise Frank Wolfe by measuring attack success rate and average iterations required for convergence.

3.1 Frank-Wolfe

Algorithm 1 FW for adversarial attacks

Require: maximum iterations T, step-sizes $\{\gamma_t\}$, convergence tolerance δ
Ensure: $y = x^n$
  1: $x_0 = x_{\text{ori}}$
  2: **for** $t = 1, ..., T$ **do**
  3:      $s_t = \arg\min_{x \in \mathcal{M}} \langle x, \nabla f(x_t) \rangle$ ▷ LMO step
  4:      $d_t = s_t - x_t$
  5:      $x_{t+1} = x_t + \gamma_t d_t$
  6:      **if** $\langle d_t, -\nabla f(x) \rangle < \delta$ **then** return   ▷ FW gap convergence criterion
  7:      **end if**
  8: **end for**

Observing oscillation in Frank Wolfe convergence is common and consequence of optimal points lying on a face of $\mathcal{M}$. Since at each iteration the method is moving towards a vertex of polytope $\mathcal{M}$, in $\mathcal{S}$, the method "zigzags", moving towards different points in effort to gradually approach the face on which the optimum lies. In the convex case, Frank Wolfe is seen to have linear complexity when optimal point x^* lies in the interior of $\mathcal{M}$, the oscillation causes sublinear convergence when x^* on the boundary. We implement variants that aim to address this problem to provide better convergence. The simplest of which is adding momentum to standard frank wolf which replaces the gradient in the LMO calculation in line (4) with a momentum term $m_t = \beta m_{t-1} + (1-\beta)\nabla f(x_t)$ and initialize $m_0 = \nabla f(x_0)$. By considering this exponentially weighted average of gradient information, momentum variants are empirically observed to have nicer convergence.

The FW algorithm has a useful interpretation that serves as basis for the following variants: Away-Step FW and Pairwise FW. Namely that at each iteration x_t is perturbed in some direction s_t, making x_{t+1} a convex combination of x_t and s_t. We record these directions in an active set $S_{t+1} = S_t \bigcup \{s_t\}$ and observe that initially x_0 is a convex combination of of active set $S_0 = \{x_0\}$. Then by induction, x_t is a convex combination of directions in S_t, admitting coefficients α such that $x_t = \sum_{s \in S_t} \alpha_s s$. Each iteration of the FW algorithm is seen to increase or introduce the contribution of s_t in the convex combination while shrink the α coefficients of all other vertices, or atoms uniformly. The innovation of the Away-Step and Pairwise variant is to recognize contribution of "bad atoms" can prevent convergence to an optimum on the boundary. These variants more directly diminish such atoms contributions by either taking steps away from selected atoms, or transferring mass between two selected atoms at each iteration as the case with the pairwise variant.

3.2 Away-Step Frank-Wolfe

The away-step FW algorithm (AFW) defines a gap in two possible directions: the typical FW step d_t^{FW} and an away direction $d_t^{\mathrm{A}} = x_t - v_t$ where $v_t \in \arg\max_{v \in S_t} \langle v, \nabla f(x_t) \rangle$. By comparing the gaps associated with the two directions, the algorithm compares the cost of taking a typical FW step to the cost associated with moving away from active atoms in S_t. Should this gap be less than that of moving towards the Frank Wolfe direction, the influence of the selected away atom $v_t \in S_t$ will be diminished, and even dropped if the corresponding $\alpha_{v_t} \leq 0$. The α updates can be seen to be inverse for that of a normal FW step. Here influence of v_t is distributed uniformly to other active atoms. New coefficients for the convex combination are for v_t, $\alpha_{v_t} := (1 + \gamma_t)\alpha_{v_t} - \gamma_t$, and otherwise $\alpha_{v_{t+1}} := (1 + \gamma_t)\alpha_v$. The algorithm enables a "drop step" where the contribution of an atom is completely removed from the convex combination, alleviating the problem of oscillation when converging to an optimum on the boundary. This algorithm is proved to have linear convergence for convex problems

---
Algorithm 2 Away-Step FW for Adversarial Attacks

Require: maximum iterations T, step-sizes $\{\gamma_t\}$, convergence tolerance δ, $x_0 \in \mathcal{M}$

1: Define $S_0 := \{x_0\}$ with $\alpha_{x_0} = 1$
2: **for** $t = 1, ..., T$ **do**
3:     $s_t := \arg\min_{x \in \mathcal{M}} \langle x, \nabla f(x_t) \rangle$ ▷ LMO step
4:     $d_t^{\mathrm{FW}} := s_t - x_t$
5:     $v_t := \arg\max_{v \in S_t} \langle v, \nabla f(x_t) \rangle$
6:     $d_t^{\mathrm{A}} := x_t - v_t$
7:     **if** $\langle d_t^{\mathrm{FW}}, -\nabla f(x) \rangle < \delta$ **then** return x_t ▷ FW gap convergence criterion
8:     **end if**
9:     **if** **then**$\langle d_t^{\mathrm{FW}}, -\nabla f(x) \rangle < \langle d_t^{\mathrm{A}}, -\nabla f(x) \rangle$
10:        $d_t = d_t^{\mathrm{FW}}, \gamma_{\max} := 1$
11:     **else**
12:        $d_t := d_t^{\mathrm{A}}, \gamma_{\max} := \frac{\alpha_{v_t}}{1 - \alpha_{v_t}}$
13:     **end if**
14:     $x_{t+1} = x_t + \gamma_t d_t$
15:     Update α, S_{t+1} s.t. $\langle \alpha, S_{t+1} \rangle = x_{t+1}$ (See below)
16: **end for**

3.3 Pairwise Frank-Wolfe

Pairwise Frank-Wolfe (PFW) is similar to AFW in that it computes the same away step. However, step taken by the algorithm is not a choice between the two, but rather their sum $d_t^{\mathrm{PFW}} = d_t^{\mathrm{FW}} + d_t^{\mathrm{A}} = s_t - v_t$.

Algorithm 3 Pairwise FW for Adversarial Attacks

Require: maximum iterations T, step-sizes $\{\gamma_t\}$, convergence tolerance δ, $x_0 \in \mathcal{M}$

1: Define $S_0 := \{x_0\}$ with $\alpha_{x_0} = 1$
2: **for** $t = 1, ..., T$ **do**
3:     $s_t := \arg\min_{x \in \mathcal{M}} \langle x, \nabla f(x_t) \rangle$ ▷ LMO step
4:     $d_t^{\mathrm{FW}} := s_t - x_t$
5:     $v_t := \arg\max_{v \in S_t} \langle v, \nabla f(x_t) \rangle$
6:     **if** $\langle d_t^{\mathrm{FW}}, -\nabla f(x) \rangle < \delta$ **then** return x_t ▷ FW gap convergence criterion
7:     **end if**
8:     Require: $\gamma_t \le \alpha_{v_t}$
9:     $d_t := s_t - v_t$
10:     $x_{t+1} = x_t + \gamma_t d_t$
11:     Update α, S_{t+1} s.t. $\langle \alpha, S_{t+1} \rangle = x_{t+1}$ (See below)
12: **end for**

The behavior of the of PFW can be understood to be transferring mass in the convex combination from the worst atom to the active set to the atom corresponding the the FW direction. At each iteration the α coefficients are

updated as follows: $\alpha_{v_{t+1}} = \alpha_{v_t} - \gamma_t$, $\alpha_{s_{t+1}} = \alpha_{s_t} + \gamma_t$ and all other α values are unchanged. To maintain x_t *convex* combination of atoms in active set, and consequently not affine or infeasible, its required $\gamma_t \leq \gamma_{\max} := \alpha_{v_t}$. By directly minimizing, and potentially dropping bad atoms from the active set, the oscillation observed with FW is mitigated. In the convex case this has been shown to give the PFW variant a linear convergence rate.

4 Results

Algorithms were tested on three pre-trained models, each performing a classification task on a different dataset. An implementation of LeNet5 [7, 8] is a CNN with 62,706 parameters trained on the MNIST dataset to classify handwritten didgets. Secondly we found a medium sized CNN pre-trined for the Fashion-MNIST dataset [9, 1]. Designed to be a more difficult problem than MNIST, the model classifies images as one of T-shirt/top, Trouser, Pullover, Dress, Coat, Sandal, Shirt, Sneaker, Bag, Ankle boot. Finally, ResNet-20 [3] is a comparatively large CNN with 20 layers. We use a pre-trained implementation adapted for the CIFAR-10 dataset [4] which classifies 3x32x32 color examples into one of 10 categories: Airplane, Automobile, Bird, Cat, Deer, Dog, Frog, Horse, Ship, and Truck. All three proved susceptible to Adversarial attacks created by FW methods to varying degrees. Representative successful attacks are shown in figure 1.
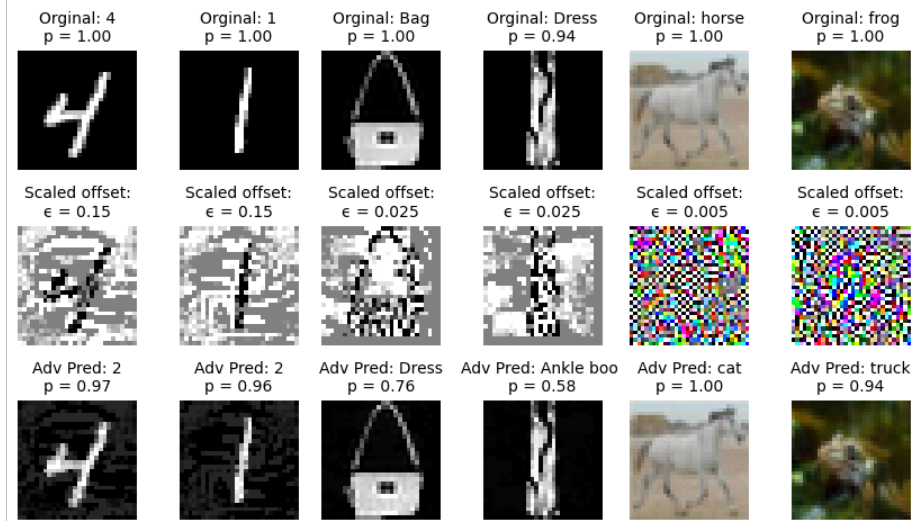

Figure 1: Representative attacks on LeNet, FMNIST, and ResNet-20.

We observed that the larger and more complicated a model, the more susceptible it is to adversarial attack. LeNet5 being a notably small and simple

model by contemporary standards, showed remarkable robustness and required attacks well within perceptible levels ($\epsilon \approx 0.3$) before the tested FW methods could reliably produce adversarial examples. While ResNet and FMNIST model can be reliably attacked with ϵ above 0.07 and 0.05 respectively (see Figure 2).

4.1 ϵ Choice

Our three different models where retrained on datasets with differing image scales. To allow for comparison of the sensitivity of each model to attacks with different ϵ, at each iteration we normalize to ensure images x_0 have mean 0.5 and variance 1 to ensure equal relative perturbation of the same ϵ on all three models.
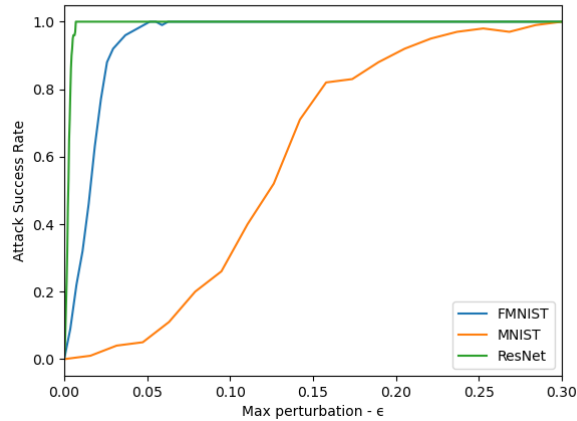

Figure 2: Effect of ϵ on attack success for untargeted FW for each dataset with L_∞ constraint.

As figure 5 shows, the different models have vastly different sensitivities to adversarial attacks. LeNet is the most robust of the three requiring large maximum perturbations for reliable attacks. The larger, more complex models can be reliably attacked with imperceptible examples in the case of ResNet or borderline perceptible in the case of the FMNIST model. Representative attacks are shown in figure 2.

4.2 Targeted vs. Untargeted Attacks

We implemented both untargeted and targeted attacks, requiring defining a custom loss function for the pre-trained models. where $f(x) = -\ell(x, y)$ for untargeted attacks, and $f(x) = \ell(x, y_{\text{adv}})$ where y is the true label and y_{adv} the adversarial target class chosen at random to be any class other than y. We find, unsurprisingly, that targeted attacks are invariably a more challenging problem,

7

resulting in lower success rates and higher average iterations for all variants and datasets.

For example, attacks on a set of 100 examples with ResNet-20 and $\epsilon = 0.005$ with normal FW algorithm using decaying rule, achieved a success rate of 0.93 requiring 5.44 iterations on average in the untargeted case, but a success rate of 0.63 and 13.26 iterations in the targeted case.

4.3 L_∞ vs L_2 Constraints

We implement attacks Linear Minimization oracles to enable both L_∞ and L_2 constrained attacks. Choices of ϵ for the two norms are clearly not comparable as L_∞ is concerned by the maximum perturbation a pixel is perturbed by, doing nothing to disincentives most if not all pixels from being perturbed, where L_2 constrains the sum of squares of perturbations.
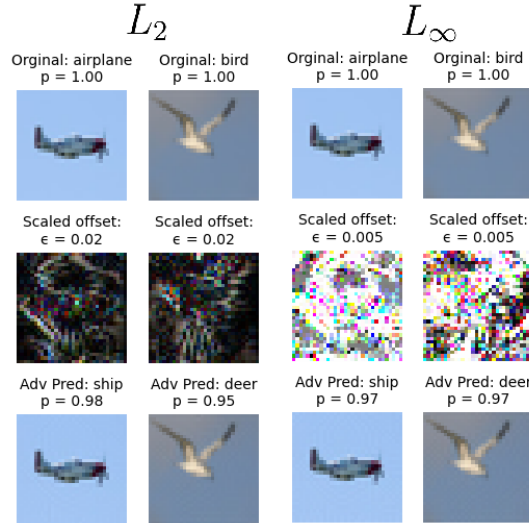

Figure 3: Effect of constraint norm on magnitude of perturbations.

To compare the resulting adversarial examples generated by attacks I chose ϵ values that gave approximately the same attack success rate of about 62% on CIFAR-10 ($\epsilon_\infty = 0.005, \epsilon_2 = 0.02$) and compare the $L1$ norm of the generated perturbations. In order to get the same success rate we expected see that $L2$ constrained attacks are more efficient at producing attacks, with an average $L1$ of 6.84 ($\sigma = 0.69$) where L_∞ constrained attacks created attacks with average perturbation L_1 of 10.5. However, we note that both cases produced attacks below with marginal perceptibility with L_2 attacks having an average L_∞ of 0.013 and it being difficult to think of applications were this efficiency is worth the trade off. We also observe, that it takes longer on average for L_2 constrained attacks to converge. Normal FW took 12.71 in L_∞ case and 13.2 for the L_2

case. From our testing we did not see any pirticular varient disproportionately affected by the choice of norm. We visualize the magnitude of attacks made by the attacks using the different constraints in figure 3.

4.4 Step-size

The methods for step-size were implemented as follows: Decaying step-size, where the step-size decreases over time according to $\gamma_t = \frac{2}{t+2}$; exact line-searching, which solves the optimization problem $\text{argmin}_\gamma f(x + \gamma d_t)$ where $\gamma \in (0, \gamma_t^{\max}]$; and Armijo-rule search, which defines stepsizes for each iteration k: $\gamma_t = \delta^k \gamma_t^{\max}$ and tests for satisfactory decrease in the objective relative to the step-size as captured by the the Armijo condition $f(x + \gamma_t d_t) \leq f(x) + \beta\gamma_t\langle\nabla f(x), d_t\langle$, where $\delta \in (0,1)$ and $\beta \in (0, 0.5)$ are fixed parameters that controll the step-size decrease at each iteration, and the desired improvement respectively. This method is well suited to this application, as it aims to provide the convergence benifits provided by adaptive step-sizes while drastically reducing queries to the loss function which is expensive in the context of adversarial attacks.

We found the application of line-searching techniques to be marginally benifit attack success rate, and appreciably decrease iterations required to converge. On a consumer grade machine and without parallizing model queries, we show the results of the three different algorithims. Where exact-LS tests 50 equally spaced stepsizes $\gamma_t \in (0, \gamma_t^{\max}]$, and Armijo rule used parameters we found to perform well through experimentation: $\gamma = 0.5, \beta = 0.5$.

Step Rule	ASR (%)	Avg. Iters	Attacks/Second
Decay	62.4	13.52	4.5
Armijo	63.6	13.13	2.5
Exact-LS	63.8	12.98	0.34

Table 1: Attack Success Rate (ASR) for PFW and Attacks/Second for Different Step Rules

4.5 Momentum

Momentum proved highly effective at reducing the number of iterations required for convergence with minimal effect attack success rate. On a test of 500 examples from CIFAR-10. Normal FW provided an ASR of 65.4% with average of 12.78 iterations. FW with momentum ($\beta = 0.8$) achieved 66.6% ASR and 9.81 mean iterations, indicating a significant improvement in convergence (see Figure 4). This is seen to outperform all other varients with the same parameters, achieving appreciably better ASR and substantially better mean convergence time.
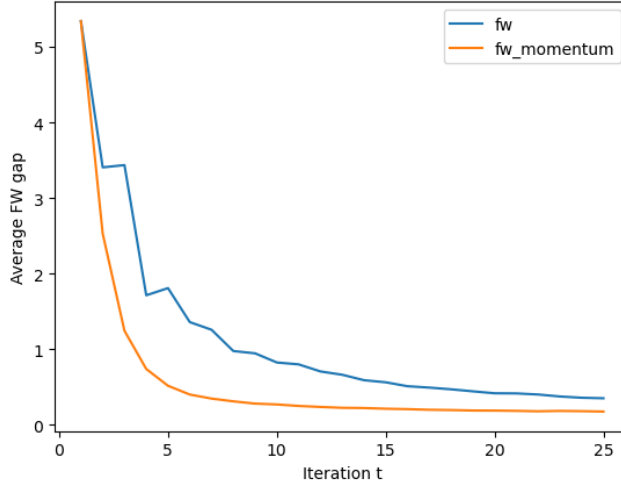
Figure 4: Comparison of g_t^{FW} of FW and momentum varient targeted attacks on ResNet-20 with $\epsilon = 0.007$ and $\beta = 0.8, N = 500$.

4.6   Variants

Algorithm	MNIST $\epsilon = 0.16$		F-MNIST $\epsilon = 0.04$		CIFAR-10 $\epsilon = 0.005$	
	ASR (%)	Avg Iter	ASR (%)	Avg Iter	ASR (%)	Avg Iter
FW	62.2	16.27	67.6	16.35	66.0	12.71
AFW	62.2	16.27	67.8	16.35	65.0	12.8
PFW	56.2	16.78	62.2	17.03	64.0	13.48

Table 2: Attack Success Rate (ASR) and Average Iterations of Frank-Wolfe Algorithm and Variants for Targeted Adversarial Attacks on 500 Examples from Three Datasets with 20 maximum iterations and decaying step-size rule.

We note that ϵ values were chosen to create a difficult optimization problem that highlighted differences in convergence between algorithms, and ϵ could have been easily chosen to ensure 100% ASR on all datasets.

We observe that the difficulty of the optimization problem, as influenced by the choice of dataset to attack, ϵ choice, and performing either targeted or untargeted attacks will effect the number of Away Steps taken by AFW. Targeted attacks on CIFAR-10 as described in table 2. For Both attacks on LeNet5 and FMNIST model, AFW was never seen to take an away step. However, when attacking ResNet-20, it is seen to have taken Away Steps 17.1% of the time. As it takes majority FW steps, the convergence of AFW is seen to closely follow that of normal FW (see Figure 5).
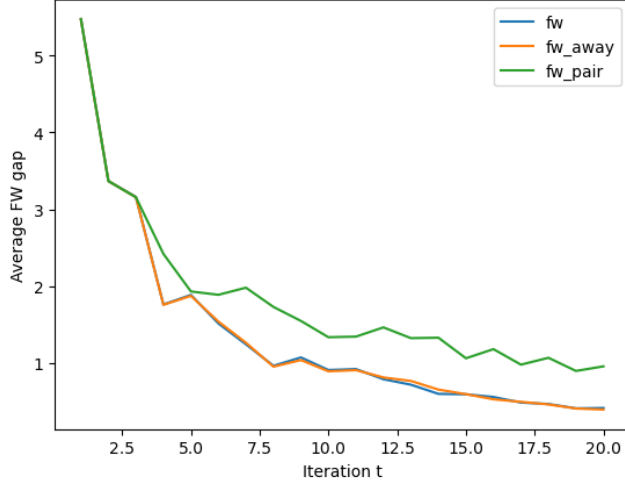
Figure 5: Average g_t^{FW} for each Algorithm by Iteration for Targeted Attacks on ResNet-20 (CIFAR-10) with decaying rule and $\epsilon = 0.005$.

5 Conclusion

Our testing with Frank-Wolf has shown it very well suited for Adversarial attacks on DNNs. We have demonstrated several factors that influence the difficulty of the optimization probelm, including choice between L_1 and L_2 constraints, choice of ϵ. Varients most often produce nearly identical perturbations, This provides some indication as to the stability of the optimization probelm. We suspect that the lack of significant improvent through the use of AFW and PFW varients is, thus not attrbutable to the non-convex nature of the problem, but trather the We observe that this application does not favor the use of PFW.

6 Convergence Analysis

The convergence of the FW algorithms in this application is complicated by the non-convexity of the DNN objective function. We reproduce a proof from Lacoste-Julien [5] for the sub-linear convergance of FW in the non-convex case. The sublinear rate of the momentum varient has an elegant proof from Chen et. al. [2]. We comment on the intuition behind the two varients (AFW and PFW) acheiving linear rates in the convex case. For the following proof we assume that f has L-Lipschitz continuous gradient on $\mathcal{M}$. This is to say that

$$f(y) \leq f(x) + \nabla f(x)^T (y - x) + \frac{L}{2} \|y - x\|_2^2$$

. This has been shown to be a reasonable assumption for DNN. Lipshitz continuous gradient gives us bound on curvature constant C_f Where C_f is the smallest

11

constant such that We additionally require that our constraint space $\mathcal{M}$ is convex and compact with diameter D. Satisfying $||x - y||_2 \leq D$ for $x, y \in \mathcal{M}$. This is trivially satisfied in the application of adversarial attacks, considering the definition of $\mathcal{M}$. Where Chen et al. 2020 used this strategy to prove the convergence of FW with momentum. We the result holds for normal FW. At each iteration since $s_t \in \mathcal{M}$, we get that $||\nabla f(x_t) - s_t||_2$

6.1   Frank-Wolfe

6.2   Pairwise Frank-Wolfe

6.3   Away-Step Frank-Wolfe

References

[1] Junaid Ali. pytorch-fashionmnist-tutorial, n.d. https://github.com/junaidaliop/pytorch-fashionMNIST-tutorial.

[2] Jinghui Chen, Jinfeng Yi, and Quanquan Gu. A frank-wolfe framework for efficient and effective adversarial attacks. *CoRR*, abs/1811.10828, 2018.

[3] Kaiming He, Xiangyu Zhang, Shaoqing Ren, and Jian Sun. Deep residual learning for image recognition, 2015.

[4] Alex Krizhevsky. Learning multiple layers of features from tiny images. 2009.

[5] Simon Lacoste-Julien. Convergence rate of frank-wolfe for non-convex objectives, 2016.

[6] Simon Lacoste-Julien and Martin Jaggi. On the global linear convergence of frank-wolfe optimization variants, 2015.

[7] Y. Lecun, L. Bottou, Y. Bengio, and P. Haffner. Gradient-based learning applied to document recognition. *Proceedings of the IEEE*, 86(11):2278–2324, 1998.

[8] Paperspace User: Nouman. Writing lenet-5 from scratch in python, 2022. https://blog.paperspace.com/writing-lenet5-from-scratch-in-python/.

[9] Han Xiao, Kashif Rasul, and Roland Vollgraf. Fashion-mnist: a novel image dataset for benchmarking machine learning algorithms, 2017.